

Figure 1. X-ray structure of complex **7b** showing partial atom labeling scheme. The third chloride anion (not shown) makes up part of the general lattice structure and is not proximate to the macrocycle. One bipyrrrole is twisted (dihedral angle = 123.3°) so that the two NH groups (N2 and N3) are oriented in nearly opposite directions. Dashed lines indicate short N—H...X contacts with relevant distances and angles: Cl2...N1 3.105 Å, Cl...H—H 156°; O2...N2 2.747 Å, O...H—N 166°; O1...N3, 2.854 Å, O...H—N 169°; Cl1...N4, 3.112 Å, Cl...H—N 132°; Cl1...N5 3.186 Å, Cl...H—N 170°; Cl2...N6, 3.175 Å, Cl...H—N 151°. Thermal ellipsoids are scaled to the 30% probability level; most H atoms have been omitted for clarity.

raaryloctaalkylporphyrins¹⁷ as well as to simplified procedures used to prepare octaalkylporphyrins.¹⁸

In our hands, the rosarin-forming reaction of Scheme I is best performed in dry CH₂Cl₂ containing a catalytic amount of TFA (12 h, room temperature, exclusion of light and air) followed by oxidation with 3 equiv of DDQ. After filtration through Celite, the product is purified by column chromatography on silica gel (3% MeOH in CH₂Cl₂, eluent) followed by recrystallization from CHCl₃/hexane to give a green metallic solid (**7a**) in surprisingly high yield (≥70%). This material, which is red-purple in solution, can be converted to the free-base form (corresponding to **2**) by treating it with 10% aqueous NaOH; treatment with aqueous HCl generates the hydrochloride salt (**7b**). This free-base, like the starting salt, appears to be stable under normal laboratory conditions.

Three different oxidation states, represented by structures **2–4**, can be formulated for the cyclic, hexapyrrolic products formed from the oxidative condensation of bipyrrrole **5** with benzaldehyde. While two of these (i.e., **3** and **4**) correspond to formal 4*n* + 2 aromatic species, we believe that it is actually the nonaromatic, *but fully conjugated*, 24*π*-electron species **7** (corresponding to structure **2**) that is formed under the reaction conditions. This assignment is based on the observation of a considerably red-shifted Soret-like transition in the UV/vis absorption spectrum of **7b** ($\lambda_{\text{max}} = 552.5 \text{ nm}$; $\epsilon = 192\,000 \text{ M}^{-1} \text{ cm}^{-1}$), which would be expected for a deformed, nonplanar structure,¹⁷ as well as an absence of any substantial ring current effects in the ¹H NMR spectrum. Moreover, as would be expected for such a 24*π*-electron formulation, the mass spectrum of the fully protonated macrocycle **7b** is consistent with a free-base structure containing three imine-type C—N bonds and three pyrrolic protons within the core.

Confirmation of the above assignment came from single-crystal X-ray diffraction analysis of the hydrochloride salt **7b**.¹⁹ The structure obtained (Figure 1) revealed the presence of three

chloride counteranions. This counteranion count is only consistent with an overall +3 charge on the macrocycle and hence serves to confirm inter alia the proposed 24*π*-electron formulation. In addition, as expected, the molecule was found to be nonplanar. Nonetheless, the system appears conjugated with the hybridization, in particular, of the three "meso-like" carbons being best assigned as sp² (as judged from bond angles). Thus, compound **7** and its free-base derivative bear closer analogy to the 20*π*-electron isophlorins²⁰ than to the 18*π*-electron porphyrins in the tetrapyrrolic series.

The procedure reported here appears to be quite general. In fact, we have found that a range of aryl aldehydes may be used in place of benzaldehyde **6a**. In all cases, however, it is the nonaromatic products (e.g., compounds **8–10**²¹) that are produced. This result, which could reflect unfavorable ethyl-phenyl interactions about the mesolike positions and/or destabilizing methyl-methyl interactions within the bipyrrrole subunits, leads us to predict that it may be possible to prepare aromatic analogues of compounds **7–10** (corresponding to structures **3** and **4**) by the judicious choice of bipyrrrole and/or aldehyde precursor. We are exploring this possibility.

Acknowledgment. This work was supported by NIH Grant AI 28845 to J.L.S. and by more recent funding from Pharmacyclics Inc. and the NSF. J.L.S. also thanks the Camille and Henry Dreyfus Foundation for a Teacher-Scholar Award (1988–1992). V. Lee thanks Prof. J.P. Collman for allowing the informal collaboration that made possible his contributions to this project.

Supplementary Material Available: Listings of synthetic experimental data for compounds **7–10** and their corresponding free-base derivatives, details of the X-ray experiment and tables of atomic thermal factors, positional parameters, bond distances, and angles for **7b**, atom labeling scheme for **7b**, side view of **7b**, and a unit cell packing diagram (29 pages); table of observed and calculated structure factor amplitudes for **7b** (44 pages). Ordering information is given on any current masthead page.

(20) Isophlorin itself is still unknown. Tetra-*N*-methylisophlorin, however, has recently been synthesized: Pohl, M.; Schmickler, H.; Lex, J.; Vogel, E. *Angew. Chem., Int. Ed. Engl.* 1991, 30, 1693–1697.

(21) Satisfactory ¹H and ¹³C NMR and high-resolution mass spectrometric data were obtained.

High-Resolution Chemical Shift and Chemical Shift Anisotropy Correlation in Solids Using Slow Magic Angle Spinning

Zhehong Gan

Molecular Spectroscopy Laboratory
School of Chemical Science, University of Illinois
Urbana, Illinois 61801

Received April 13, 1992

In this communication, a new and simple two-dimensional NMR method is presented to obtain high-resolution chemical shift and chemical shift anisotropy correlation spectra of solids. This method can be easily implemented without additional hardware on normal magic angle spinning probes using very low spinning rates.

Magic angle spinning (MAS) has been used as the standard method to obtain high-resolution NMR spectra of solids.¹ When the chemical shift anisotropy (CSA) is large compared with the spinning rate, MAS spectra are often crowded with spinning sidebands which make the line assignments and the quantitative analysis of the spectra difficult. This problem is further intensified on high-field NMR spectrometers because of the increased magnitude of the CSA.

(1) Schaefer, J.; Stejskal, E. O. *J. Am. Chem. Soc.* 1976, 95, 1031.

(17) Barkigia, K. M.; Berber, M. D.; Fajer, J.; Medforth, C. J.; Renner, M. W.; Smith, K. M. *J. Am. Chem. Soc.* 1990, 112, 8851–8857.

(18) Sessler, J. L.; Mozaffari, A.; Johnson, M. R. *Org. Synth.* 1991, 70, 68–77.

(19) Rosarin **7b**: (C₆₃H₆₉N₆³⁺)(Cl⁻)₃·4H₂O·2CHCl₃; triclinic, *P* $\bar{1}$ (No. 2), *Z* = 2 in a cell of dimensions *a* = 11.8030 (13), *b* = 14.813 (2), *c* = 20.826 (2) Å, α = 81.520 (9), β = 74.541 (9), γ = 77.382 (9)°, *V* = 3387.3 (6) Å³, ρ_{calcd} = 1.30 g cm⁻³ (188 K), *F*(000) = 1392. Data were collected at 188 K on a Nicolet P3 diffractometer; the final *R* = 0.0688, *wR* = 0.0810, and goodness of fit = 2.268 for 763 parameters. For details see the supplementary material.

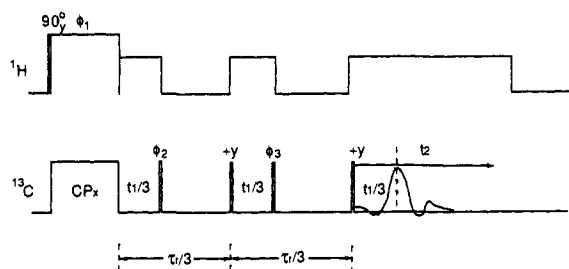


Figure 1. Pulse sequence of the chemical shift and CSA correlation experiment using slow magic angle spinning. The last segment of the evolution period is incorporated into the acquisition period, and all of the narrow pulses are 90° pulses.

Table I. Phase Cycle Used in the 2D Chemical Shift and CSA Correlation Experiment.

step	ϕ_1	ϕ_2	ϕ_3	receiver	blocks
1	+x	-y	-y	+x	real
2	+x	+x	-x	+x	real
3	+x	-y	+x	+x	imaginary
4	+x	+x	-y	+x	imaginary

^a The simultaneous phase alternation (+x and -x) of the spin-lock phase ϕ_1 and the receiver phase can be added to the listed phase cycle.

The magic angle hopping experiment introduced by Bax et al.² shows a different approach to narrow spectral lines of solids by using discrete sample hopping about the magic angle. The experiment results in a two-dimensional (2D) isotropic chemical shift and CSA correlation spectrum, and it has the advantage that there is no spinning sideband in the high-resolution spectrum. The useful CSA information can be obtained from the CSA powder pattern line shapes³ along the second dimension in the 2D spectrum. The experiment requires a fast and accurate mechanical hopping system which limits the application of this technique.

The method presented in this communication uses continuous slow magic angle spinning to replace the discrete hopping in the magic angle hopping experiment. As shown by the pulse sequence in Figure 1, the evolution period of this 2D method is divided into segments spaced by one-third of a rotor cycle. During the time between these evolution segments, the magnetization of the sample is stored along the external magnetic field while the sample is rotated 120° about the magic angle. The chemical shift for each segment is the sum of the isotropic chemical shift and a contribution from the CSA. This CSA contribution is different in each segment due to the different orientations of the sample with respect to the external magnetic field. The net contribution from CSA for three evolution segments is simply averaged to zero due to the nature of the second rank tensor for the chemical shielding.² In the case of spinning samples, it has been shown that the net evolution of the magnetization for the three evolution segments depends only on the isotropic chemical shift and is independent of the CSA and the spinning rate.⁴ Thus, without the CSA broadening during the evolution period, an echo forms at the end of the third segment as shown in Figure 1. The isotropic chemical shift and CSA correlations can be obtained by acquiring the CSA powder patterns in the t_2 period.

The 2D experiment is acquired in the hypercomplex phase-sensitive manner⁵ with the phase cycle listed in Table I. Thus, the spectrum is purely absorptive in both dimensions. As shown in Figure 1, the acquisition period is started immediately after the last pulse instead of at the top of the echo. This modification increases the sensitivity of the method for two reasons: First, a

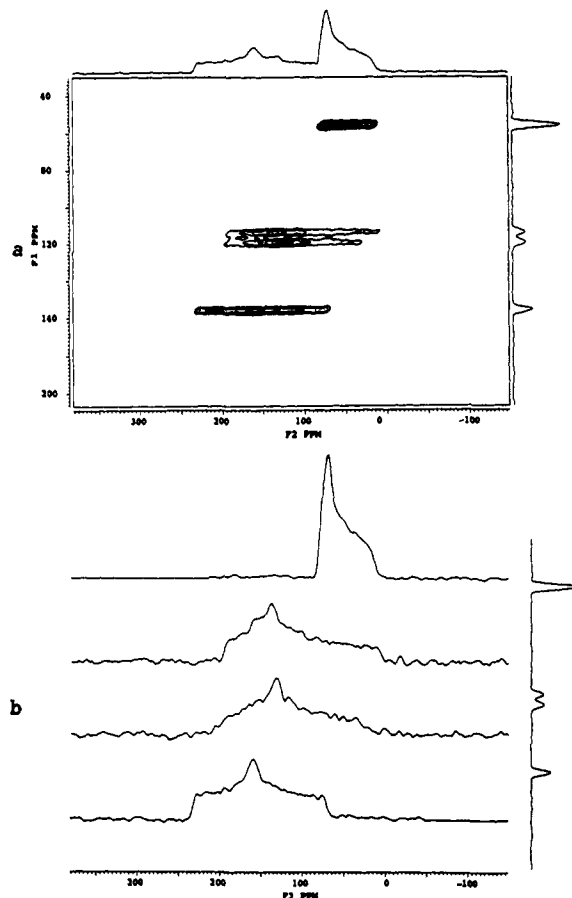


Figure 2. (a) Chemical shift and CSA 2D spectra of 1,4-dimethoxybenzene after processing with spectra shearing. The spectra were recorded on a General Electric GN-300 spectrometer (^{13}C frequency of 75.46 MHz). A Chemagnetics MAS probe with a 7.5-mm pencil type spinner (spun at 100 ± 2 Hz) was used for the measurement. A total of 128 blocks of data (64 complex blocks) were recorded with a 4.8-ms acquisition time for the t_1 dimension. With a 5-s repetition delay and 24 scans for each block, it takes a total of 4.3 h to acquire the data. (b) Resolved CSA powder patterns.

full echo is acquired rather than only half of the echo. Second, it takes only half of the scans to acquire the same signal intensity as compared to starting the acquisition at the top of the echo.⁴ However, the spectra obtained by this modification must be tilted or sheared by an angle of $\tan^{-1}(1/3)$ to provide the chemical shift and CSA correlation spectra. This type of shearing or tilting has commonly been used in 2D homonuclear J spectra in solution.⁶

Figure 2 presents the 2D chemical shift and CSA correlation spectra of 1,4-dimethoxybenzene. After the spectral shearing, the projection along the t_1 dimension shows the high-resolution isotropic chemical shift spectrum. All of the peaks are well resolved, even for the two protonated aromatic carbons which are separated by less than 5 ppm. The height of the peaks in the projection depends on the CSA; however, the peak volume under each CSA powder pattern in the 2D spectra can be used for quantitative analysis. The three principal elements of the chemical shielding tensor for each spin can be easily obtained from each individual CSA powder pattern projected along the t_2 dimension as shown in Figure 2b.

The experiment of 1,4-dimethoxybenzene clearly demonstrates that high-resolution spectra can be obtained using very slow magic angle spinning by this simple method. The low spinning rate requirement and the absence of spinning sideband of this method allow one to increase the sensitivity by using large volume samples and high-field spectrometers, thereby shortening the time required

(2) Bax, A.; Szevernyi, N. M.; Maciel, G. E. *J. Magn. Reson.* **1983**, *52*, 147.

(3) Mehring, M. *High Resolution NMR of Solids*; Springer-Verlag: New York, 1983. Haeblerlin, U. *High Resolution NMR of Solids Selective Averaging*; Academic Press: New York, 1983.

(4) Gan, Z. Manuscript in preparation.

(5) States, D. J.; Haberkorn, R. A.; Ruben, D. J. *J. Magn. Reson.* **1982**, *48*, 286.

(6) Nagayama, K.; Bachmann, P.; Wüthrich, K.; Ernst, R. R. *J. Magn. Reson.* **1978**, *31*, 133.

for the 2D experiment. The separation of the CSA powder patterns in a 2D spectrum removes the overlap that is often severe in the one-dimensional spectrum of a static sample, revealing the useful CSA information.

17-O-Acetyltestosterone Formation from Progesterone in Microsomes from Pig Testes: Evidence for the Baeyer-Villiger Rearrangement in Androgen Formation Catalyzed by CYP17

Amy Y. Mak and David C. Swinney*

Department of Drug Metabolism, A3-295
Syntex Research, 3401 Hillview Avenue
Palo Alto, California 94304

Received July 7, 1992

Androgens are formed by testicular cytochrome P450 CYP17¹ via an initial 17 α -hydroxylation of progesterone (P) or pregnenolone followed by the cleavage of the C-17 side chain.² Although the cleavage reaction observed in testes has been shown to utilize NADPH and molecular oxygen,³ a definitive mechanism for the reaction has evaded investigators. In this communication we report the NADPH-dependent formation of 17-O-acetyltestosterone (AT) upon incubation of P with microsomes and purified CYP17 from perinatal pig testes. The formation of AT suggests that this enzyme has the capacity to catalyze the Baeyer–Villiger rearrangement via a ferric heme peroxy substrate intermediate.

The formation of AT, 17 α -hydroxyprogesterone (17 α -OHP), and androstenedione (A) was analyzed by HPLC with a radio-flow detector. The products were eluted from a 5- μ m ODS column isocratically with 30% methanol, 25% acetonitrile, and 45% water at a flow rate of 1 mL/min.⁴ AT was identified by comigration with authentic standard (retention time 73 min) and confirmed by GCMS. Under electron impact ionization (70 eV; source temperature 150 °C), the parent compound had a molecular weight of m/z 330 with a major fragment corresponding to the loss of acetate ($M^+/-60$). No ion corresponding to the loss of water ($M^+/-18$) was observed.

In microsomes the formation rate of AT was 1 pmol/min/mg of protein as compared to 305 and 45 pmol/min/mg for 17 α -OHP and A, respectively, while the activity associated with the purified enzyme was 1.6, 447, and 326 pmol/min/nmol of P450 for AT, 17 α -OHP, and A, respectively, under the conditions described in ref 4. AT formation was NADPH-dependent in both systems.

If AT is formed by CYP17, then it and 17 α -OHP should arise from the same CYP17–progesterone complex and their rates of formation should be equally sensitive to competitive inhibitors. Ketoconazole, a well-characterized competitive inhibitor of CYP17,⁵ and pregnenolone, the cosubstrate for the reaction, did

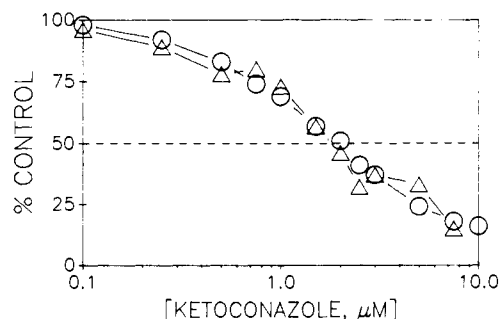


Figure 1. Inhibition of CYP17 activities in microsomes from pig testes by ketoconazole. The effect of ketoconazole upon the formation of AT (Δ) and 17 α -OHP (\circ) was determined in 10-min incubations at 37 °C containing 1.5 mg/mL of protein and 50 μ M [³H]progesterone.

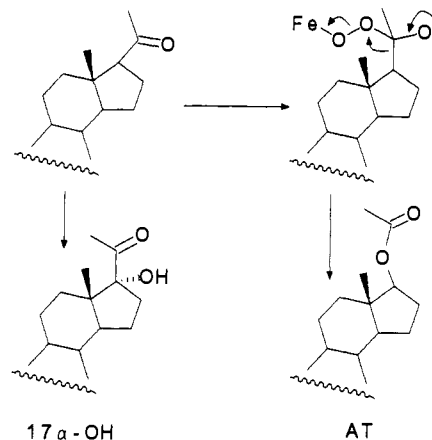


Figure 2. Proposed mechanism in the formation of 17-O-acetyltestosterone via the Baeyer–Villiger rearrangement.

not differentially inhibit the formation of either product. The IC_{50} values, associated with ketoconazole inhibition were 1.60 ± 0.74 and 2.27 ± 0.20 μ M, respectively, for AT and 17 α -OHP (Figure 1),⁶ and the apparent K_i values associated with pregnenolone inhibition (determined by the method of Dixon) were 5.0 ± 3.5 μ M for AT and 9.6 ± 4.6 μ M for 17 α -OHP. The formation of both products by purified CYP17 was inhibited 48 and 51% by 5 μ M ketoconazole, respectively. These data strongly suggest that AT is formed from the same enzyme–substrate complex as 17 α -OHP.

The insertion of an oxygen in a carbon–carbon bond is most readily accomplished via rearrangement of a peroxy intermediate. This well-characterized chemical reaction is known as the Baeyer–Villiger rearrangement.⁷ The rearrangement of the C-20 ferric peroxide of progesterone via the Baeyer–Villiger rearrangement would result in the formation of AT (Figure 2). Precedent for this type of reaction being catalyzed by a cytochrome P450 was recently shown in a report by Fisher and co-workers.⁸ They reported evidence that lanosterol 14 α -demethylase catalyzes the formation of 14 α -(formyloxy)lanost-8-en-3 β -ol from lanosterol and concluded that this could only arise via the Baeyer–Villiger rearrangement.

Since AT has not yet been shown to be an intermediate in A formation from P, it does not directly implicate this mechanism in androgen formation by CYP17. It is possible that this is a process that occurs infrequently (leakage). Reports in the literature, primarily by Akhtar and co-workers,⁹ propose the in-

* Author to whom correspondence should be addressed.

(1) CYP17 has been referred to as 17 α /20 lyase, P450_{17 α} , and P450_{SCC11}.
(2) (a) Nakajin, S.; Hall, P. F. *J. Biol. Chem.* **1981**, *256*, 3871–2876. (b) Nakajin, S.; Shinoda, M.; Haniu, M.; Shively, J. E.; Hall, P. F. *J. Biol. Chem.* **1984**, *259*, 3971–3976.

(3) Lynn, W. S.; Brown, R. H. *J. Biol. Chem.* **1958**, *232*, 1015–1030.

(4) The microsomal incubations typically contained 1.5 mg/mL of microsomal protein from pig testes, 25 μ M [³H]progesterone, 50 mM potassium phosphate (pH 7.25), 3 mM magnesium chloride, and 1 mM NADPH. The incubations with the reconstituted system contained 0.22 μ M CYP17, 5000 units/mL cytochrome P450 reductase, and 5 μ g/mL dilauroylphosphatidylcholine. CYP17, purified by the method of Suhara (Suhara, K.; Yoshiyuki, F.; Shiroy, M.; Katagiri, M. *J. Biol. Chem.* **1984**, *256*, 8729–8736), produced a single band by SDS gel electrophoresis. Cytochrome P450 reductase was purified by the methods of Dignam and Strobel (Dignam, J. D.; Strobel, H. W. *Biochem. Biophys. Res. Commun.* **1975**, *63*, 845–852) and Yasukochi and Master (Yasukochi, Y.; Masters, B. S. S. *J. Biol. Chem.* **1976**, *251*, 5337–5344).

(5) (a) Van Wauwe, J. P.; Janssen, P. A. *J. Med. Chem.* **1989**, *32*, 2231–2239. (b) Ayab, M.; Levell, M. J. *J. Steroid Biochem.* **1987**, *28*, 521–531. (c) Kan, P. B.; Hirst, M. A.; Feldman, D. *J. Steroid Biochem.* **1985**, *23*, 1023–1029.

(6) IC_{50} values are the mean \pm standard deviation from the separate experiments. Each IC_{50} value was determined by the best fit to the following equation: % of control activity = $100(1 - (S/S + IC_{50}))$. All r values were greater than 0.97.

(7) March, J. In *Advanced Organic Chemistry Reactions, Mechanisms, and Structure*; McGraw Hill Inc.: New York, 1991; 1011–1012 and references therein.

(8) Fisher, R. T.; Trzaskos, J. M.; Magolda, R. L.; Ko, S. S.; Brosz, C. S.; Larsen, B. *J. Biol. Chem.* **1991**, *266*, 6124–6132.